INTERNATIONAL JOURNAL OF CLIMATOLOGY, VOL. 15, 753–771 (1995)

PREDICTION OF THE DRY AND WET SPELL OF THE AUSTRALIAN MONSOON

T. N. KRISHNAMURTI, SANG-OK HAN AND VASUBANDHU MISRA
Department of Meteorology, Florida State University, Tallahassee, FL 32306-3034, USA

Received 1 November 1993
Accepted 14 February 1995

ABSTRACT

This study is a sequel to two recent studies on the monsoonal dry and wet spells. The previous studies addressed the dry and wet spells of the monsoon over India and China on the intraseasonal time-scales. The present study is intended to provide an outlook for the occurrence of dry and wet spells in reference to the Australian monsoon, within roughly a 1-month period from the time of start of the forecast with a global model. In the global model, the definition of a time mean state and an intraseasonal component are retained. The high-frequency component is viewed as one where inclusion in the initial state can contribute to a degradation of month long forecasts and hence is excluded initially. Sea-surface temperature anomalies on intraseasonal time-scales are included in this analysis. The prediction of the wet spells of the monsoon is assessed from the superposition of the predicted intraseasonal cyclonic circulation anomaly on top of the climatological cyclonic anomaly. The dry spell is assessed from an inverse superposition. We consider here a specific period, i.e. March 1992. The early part of this month was characterized by a wet spell over Northern Australia. A dry spell prevailed during the middle of this month and was followed by a wet spell during the latter part of the month. The prediction experiments with a prescribed and a modelled sea-surface temperature anomaly successfully demonstrated the passage of the intraseasonal anomaly, with the superposition of the geometrics of the intraseasonal and the climatic components favouring the wet and the dry spell during different periods of the month.

KEY WORDS: Australian monsoon; wet and dry spell prediction; global circulation model; 30–60 day oscillation

INTRODUCTION

This study proposes a methodology to predict the low-frequency circulations and modulations of weather over Northern Australia. This follows our two recent publications using the same prognostic methods over India (Krishnamurti *et al.*, 1990) and China (Krishnamurti *et al.*, 1992b). The premise of this study is based on the fact that superposition of intraseasonal circulation anomalies (on the time-scale of 30–60-days) and the climatological circulations favours enhanced or deficit rainfall anomalies. The passage of an anticyclonic intraseasonal circulation anomaly over a region of climatological rainfall is viewed as the one that favours below normal rainfall and vice versa. This is the type of relationship that we shall be seeking from the model simulations of the flow fields in order to assess the occurrence of dry and wet spells over the Northern Australian region. This interpretation of the relationship between the passage of intraseasonal low-frequency modes and intraseasonal rainfall anomalies for the Northern Australian region is quite analogous to our previous studies over India and China. The Arabian Sea and the Chinese components of the monsoon undergo an enhancement of the rains when the oceanic components of the flow towards the land mass enhances the on-shore circulations of the subtropical highs.

In the context of the Australian monsoon, it is the enhancement of the monsoon trough (between 10° and 15°S), which is the Intertropical Convergence Zone (ITCZ), over this region that undergoes a modulation from the passage of low-frequency modes. The importance of 30–60-day oscillations and local rainfall and westerly wind anomalies over the Australian region has been studied by Troup (1961). He noted a pronounced modulation of the monsoon westerlies coherent with rainfall anomalies on this time-scale. In our study we shall make reference to cyclonic circulation anomalies with their centre around 15°S, which carry westerly wind anomalies, enhanced

CCC 0899-8418/95/070753-19

moisture transport and rainfall on their northern flank. The alternation between cyclonic and anticyclonic circulation features over this region is associated with the alternation of westerly and easterly anomalies and a modulation of rainfall. Our study addresses the prediction of these circulation anomalies. Schematically we illustrate these parallel and antiparallel geometries for the Northern Australian wet and dry spells in Figure 1 (a and b). Here the solid lines illustrate the climatological flows, and the dashed lines show the transients, i.e. the intraseasonal component.

The proposed experiment covers the entire month of March 1992. The choice of this month for the proposed study of the 30–60-day oscillation over the Northern Australian region was motivated from a study of Stringer (1992). Stringer noted a strong relationship between the 30–60-day oscillations (as inferred from time-filtered outgoing longwave radiation data) and the occurrence of dry and wet spells over Northern Australia during this month. Power spectral analysis of cold-surge indices of the winter monsoon and of the monsoon westerly flow reveal a broad peak on this time-scale during this period (Stringer, 1992). The climatological flow field for the proposed experiments in this study is based on Atkinson (1971) and the climatological monthly mean rainfall is based on Diaz *et al.* (1989), and are illustrated in Figure 2. Basically this illustration portrays a zonally oriented axis of a cyclonic circulation belt between 10° and 15°S. This is the position of the climatological monthly mean monsoon trough. The precipitation climatology depicts a rainy region during this month over this region.

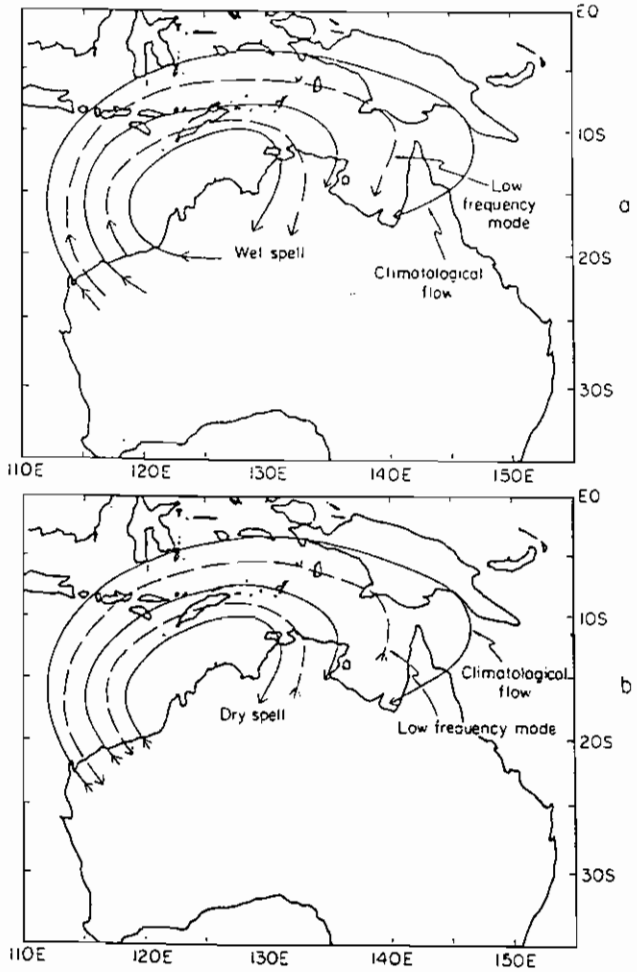

Figure 1. Schematic illustration of the flow field showing (a) parallel and (b) antiparallel flows during wet and dry spells of the monsoon over Northern Australia

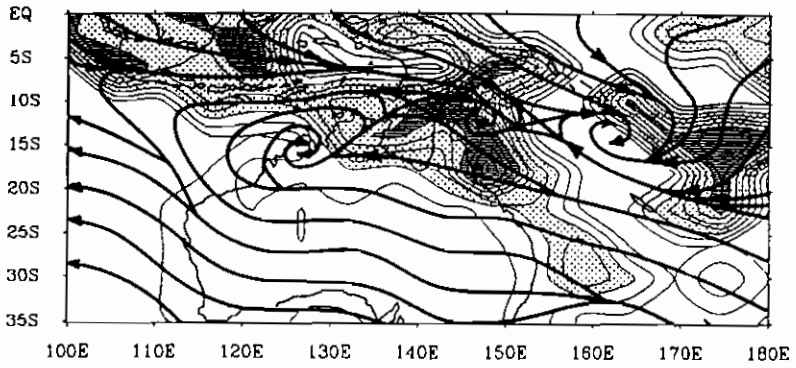

Figure 2. Climatological flow field for March based on Atkinson (1971) and climatological monthly mean rainfall field (stipled) based on Jaeger (1969). Streamlines (solid lines) and isotachs (thin lines at 25 knots interval)

In the following section we present an outline of a global model that is used to predict the position of low-frequency transients on time-scale of 30–60 days. The observed intraseasonal components are illustrated in the section following that. The methodology and results of the modelling are addressed in subsequent sections.

OUTLINE OF FSU GLOBAL SPECTRAL MODEL (FSUGSM)

The model used in the present study is a 12-layer global spectral model in the vertical (vertical coordinate being $\sigma = p/p_s$) between roughly 100 hPa and 1000 hPa. In the horizontal it has a spectral representation of T21 (triangular truncation of 21 waves). The dependent variables of the model are vorticity, divergence, vertical velocity, temperature, dewpoint depression, and the log of surface pressure. The independent variables are x, y, σ, and t. The model utilizes a semi-implicit time differencing scheme. The model includes a time filter based on Asselin (1972). Centred finite differences are used in the vertical for all variables except humidity, which is handled by an upstream differencing scheme. Fourth-order linear horizontal diffusion following Kanamitsu *et al.* (1983) is adopted. The orography is based on a mean terrain height at the resolution T21 and is extracted from a Navy data at a 10-minute resolution. The vertical boundary conditions are kinematic, with $\dot{\sigma} = 0$ at top and bottom. The model is initialized using non-linear diabatic normal mode initialization with five vertical modes (Kitade, 1983). Cumulus parameterization is based on a modified Kuo's scheme (Krishnamurti *et al.*, 1983). Surface fluxes are based on similarity theory, with vertical distribution of fluxes utilizing a mixing length formulation where the exchange coefficients are functions of the Richardson number (Louis, 1979). The ground temperature is computed from a surface energy balance over land and is coupled to the surface similarity fluxes (Krishnamurti *et al.*, 1988). A surface hydrology is included, based on Dastoor and Krishnamurti (1991). Large-scale condensation is carried out via a disposition of supersaturation (T, q). Dry convective adjustment follows Kanamitsu (1975), and shallow moist convection is based on the formulation of Tiedke and Slingo (1985). Longwave and shortwave radiation are based on band models that follow Harshvardhan and Corsetti (1984) and Lacis and Hansen (1974), respectively. Parameterizations of low, middle, and high clouds are based on threshold relative humidity for radiative transfer calculations.

OBSERVED INTRASEASONAL MOTION FIELD

In Figure 3 we illustrate the time history of the motion field at 850 hPa (time filtered) on the scale of 30–60-days. Initially this sequence shows a clockwise circulation axis, identified as a trough line, near 10°S. A ridge line was apparent over Southern Australia near 40°S. The wet areas of the Australian monsoon were noted near 10°S. The amplitude of the low-frequency wind is around 1– 3 m s^{-1}. As we go through the sequence of panels in Figure 3, which shows the motion field at 5-day intervals from day 0 to day 30, we note a meridional (southward) propagation of the trough–ridge lines. Such a southward propagation was noted previously by Comeaux (1991) and reviewed by Krishnamurti *et al.* (1992a). A wet spell extending roughly between 10°S and 20°S over parts of

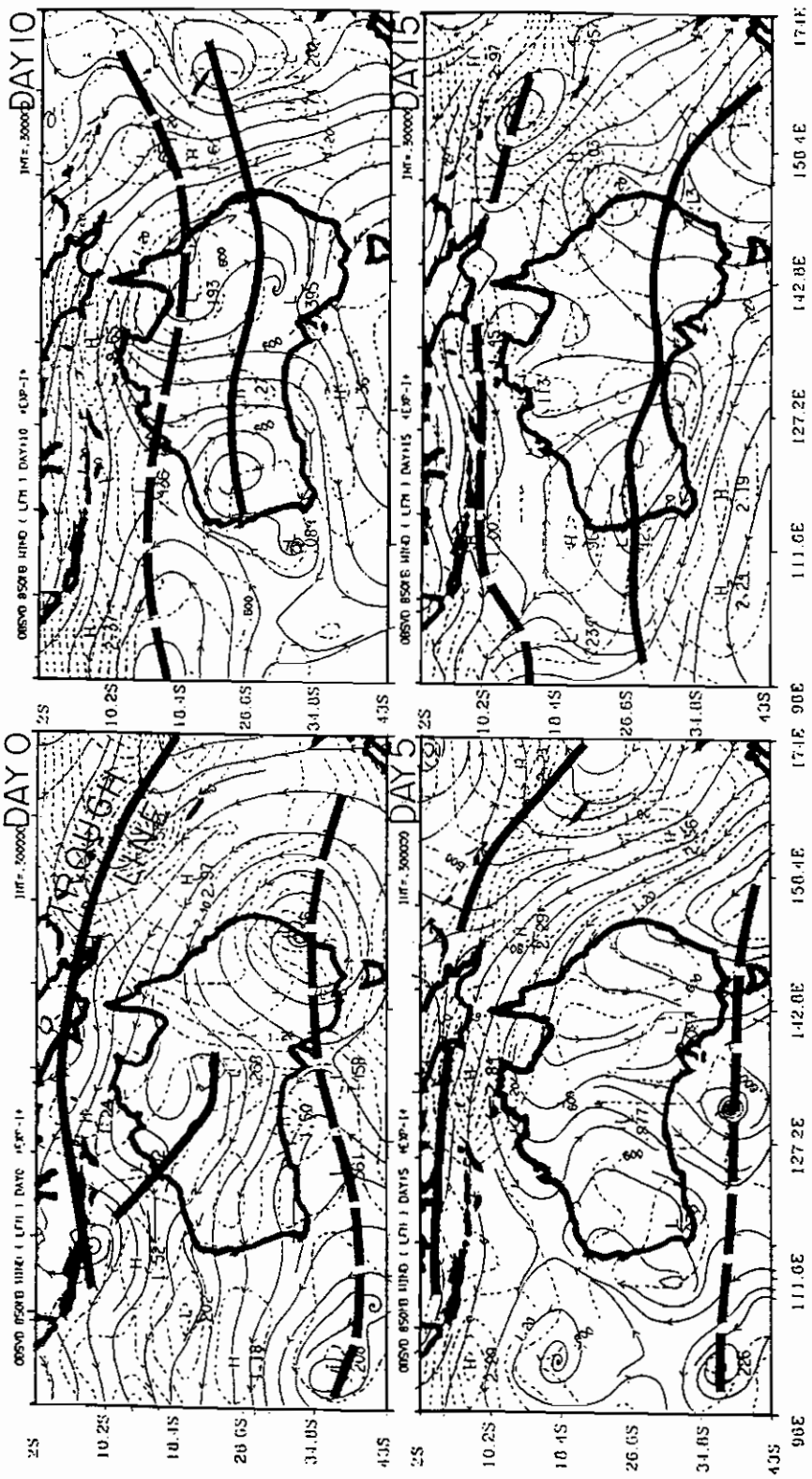
DAY 0
DAY 5
DAY 10
DAY 15
TROUGH
LINE
10.2S
18.4S
26.6S
34.8S
43S
90E
111.6E
127.2E
142.8E
150.4E

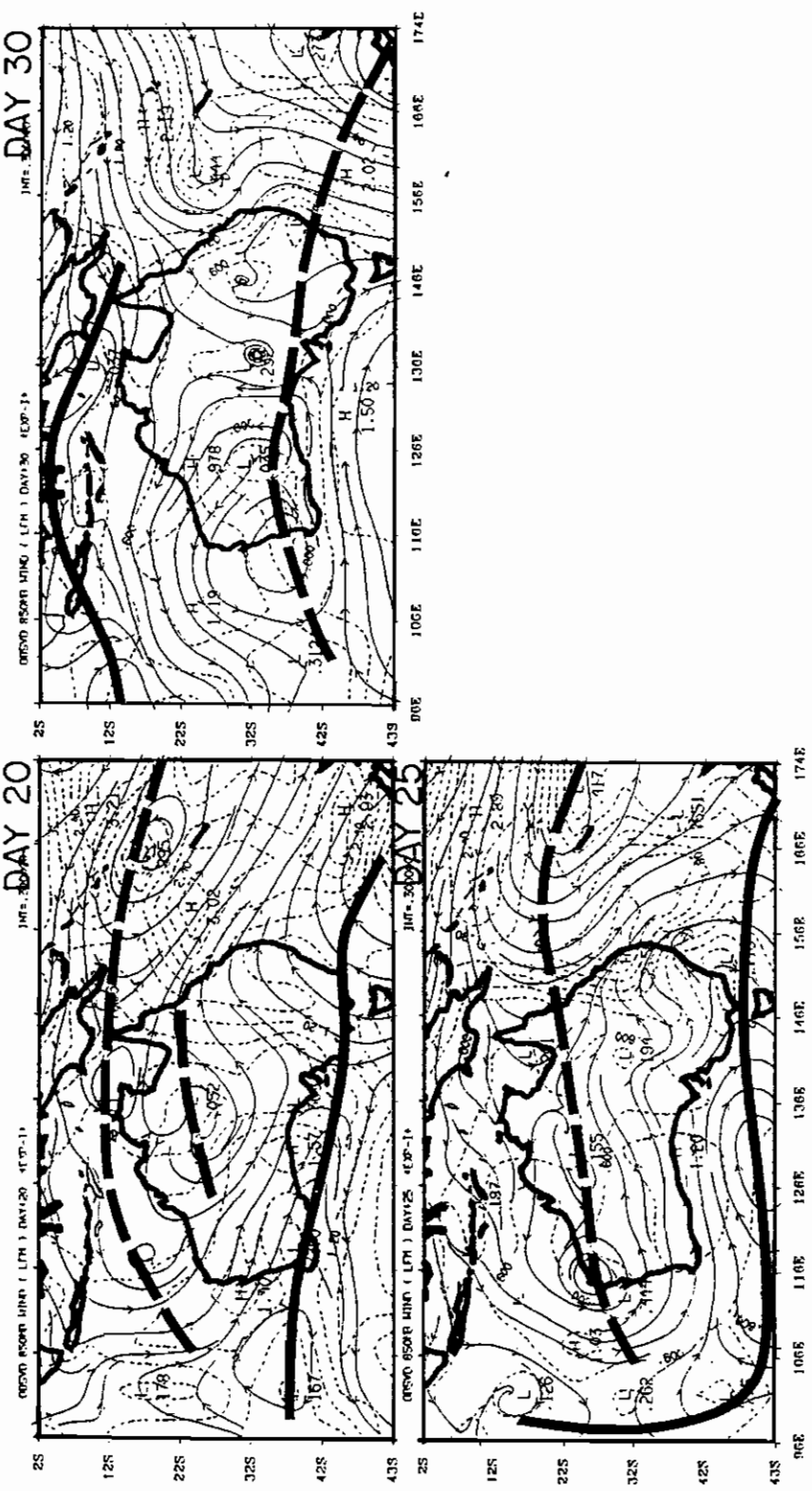

Figure 3. Observed 30–60-day time filtered flow field at 850 hPa from March 1 to March 30, 1992 at intervals of 5 days. Streamlines (solid lines) and isotachs (dashed lines) at intervals of 0·3 m s^{-1}. Thick lines are trough lines and thick dashed lines are ridge lines

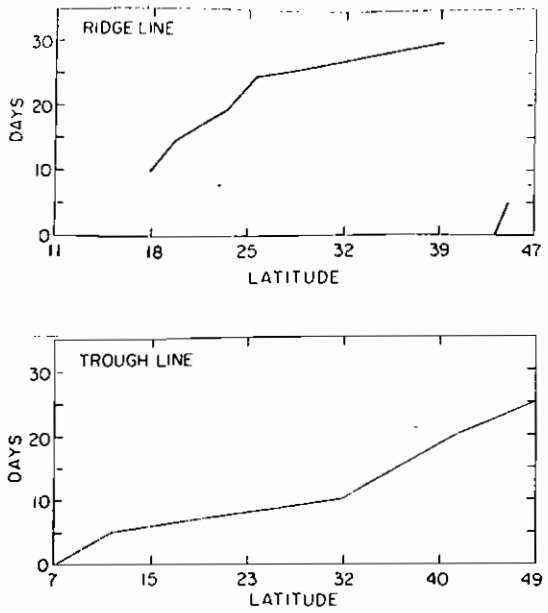

Figure 4. Low-frequency (30–60-day) modes of ridge and trough lines as observed

Northern Australia and over the Gulf of Carpenteria and the Timor Sea during early and late March was coincidental with the trough line being located near 10°S. During the period of the dry spell over this region, i.e. the middle of March, a ridge line was located near 12°S.

The southward propagation of the ridge and trough lines are best illustrated in Figure 4, derived from Figure 3. Here the zonally averaged latitudinal positions between 96°E and 174°E of the trough and the ridge are displayed. We note from the figure that the speed of the meridional motion is roughly 1·3° latitude day^{-1}. The meridional scale of this system is around 4000 km.

Around the initial time (i.e. around days 0 and 5) a ridge line was noted around 40°S, which soon moved southward and out of the domain. This was followed by the appearance of a new ridge line around 18°S by day 10.

PROPOSED EXPERIMENTS

The methodology proposed follows our previous studies (Krishnamurti *et al.*, 1990, 1992b). One of the main objectives of this study is to predict the low-frequency modes through at least one cycle, i.e. 30–60 days into the future. Towards this end the experiments were carried out with the following initial state.

(i) A time mean state for all variables at all levels defined from a period of 45 days preceding the initial time $t = 0$. This was necessary to provide an energy source for the low-frequency modes.

(ii) A low-frequency mode for all variables at all levels on the time-scale of 30–60-days was extracted from a time series of 120 days prior to the initial time $t = 0$ by using a simple recursive first-order Butterworth filter.

(iii) The long-term mean annual cycle of SST was retained throughout the time integration.

(iv) (a) One of the experiments involved prescribing the sea-surface temperature anomalies (SSTA) for the entire length of the experiment. In this experiment the SSTA on the time-scale of 30–60-days was obtained by time filtering the daily values from day −120 to day +120. This does not make the experiment entirely predictive. (Hereafter this methodology will be called experiment 1.)

(b) The other proposed experiment involved using extrapolated SSTA beyond day 0, thus making this experiment truly predictive. The time series of SSTA of 200 days prior to day 0 was subjected to Fourier transform at each grid-point. The 30–60-day modes were time filtered using the first-order Butterworth filter. The phase and amplitude of the 30–60-day frequency modes were extrapolated beyond day 0. The

results of this extrapolation were found to conform well with the observed anomalies in this time-scale. (Hereafter this prognostic method will be called experiment 2.)

Furthermore, SSTA was enhanced by a factor of 3·5, as suggested by numerous studies on climatic impact of SSTA (Krishnamurti *et al.*, 1990, 1992b). This was necessary in this study, in particular, as the 12-layer global model presently used lacked an adequate resolution for the calculation of surface fluxes of moisture, heat, and momentum in the planetary boundary layer.

SLOWING THE CONTAMINATION OF LOW FREQUENCY MOTIONS

Figures 5 (a and b) illustrates the typical error growth in these month-long integrations. Here the anomaly correlations of the 850 hPa low-frequency motion field from our previous month-long integration are shown (Krishnamurti *et al.*, 1992b). These were for the forecasts of the monsoonal dry and wet spells over India and China. In these forecasts an anomaly correlation on day 30 exceeded 0·5. However, a disturbing aspect was the rapid drop of skill during the first 120 h of integration. This was true of all of our previous experiments. This loss of skill may be due to a number of factors, such as the slow rise of amplitude of higher frequency motions and their contribution to the error growth for the low frequencies (Krishnamurti *et al.*, 1992b). This also could be a spin up (or initialization) problem—i.e., the initial time mean state plus the initial low-frequency variables simply do not

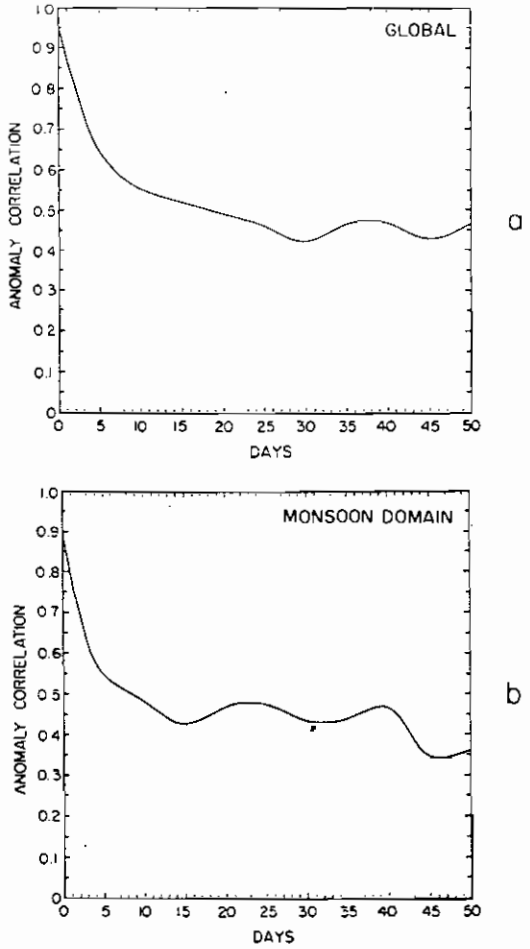

Figure 5. Typical anomaly correlations of (a) global and (b) tropical low-frequency component of 850 hPa wind (from Krishnamurti *et al.*, 1992b)

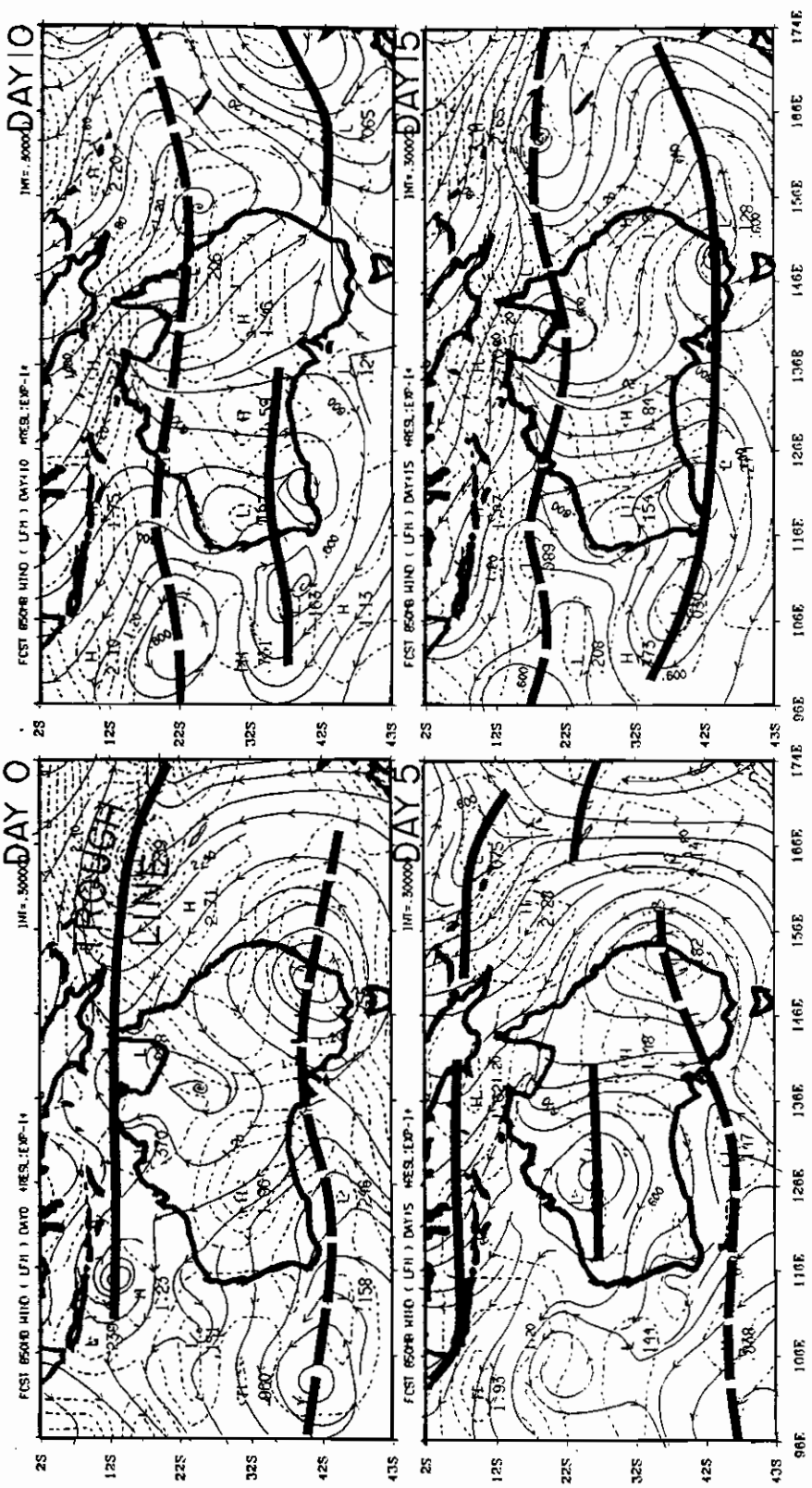
DAY 0
DAY 5
DAY 10
DAY 15
FCST 850MB WIND (LFM) DAY0 MRSL:EXP-1#
FCST 850MB WIND (LFM) DAY5 MRSL:EXP-1#
FCST 850MB WIND (LFM) DAY10 MRSL:EXP-1#
FCST 850MB WIND (LFM) DAY15 MRSL:EXP-1#
INIT=.00000
INIT=.00000
INIT=.00000
INIT=.00000
LINE
25
125
225
325
425
435
96E
106E
116E
126E
136E
146E
156E
166E
174E
180E

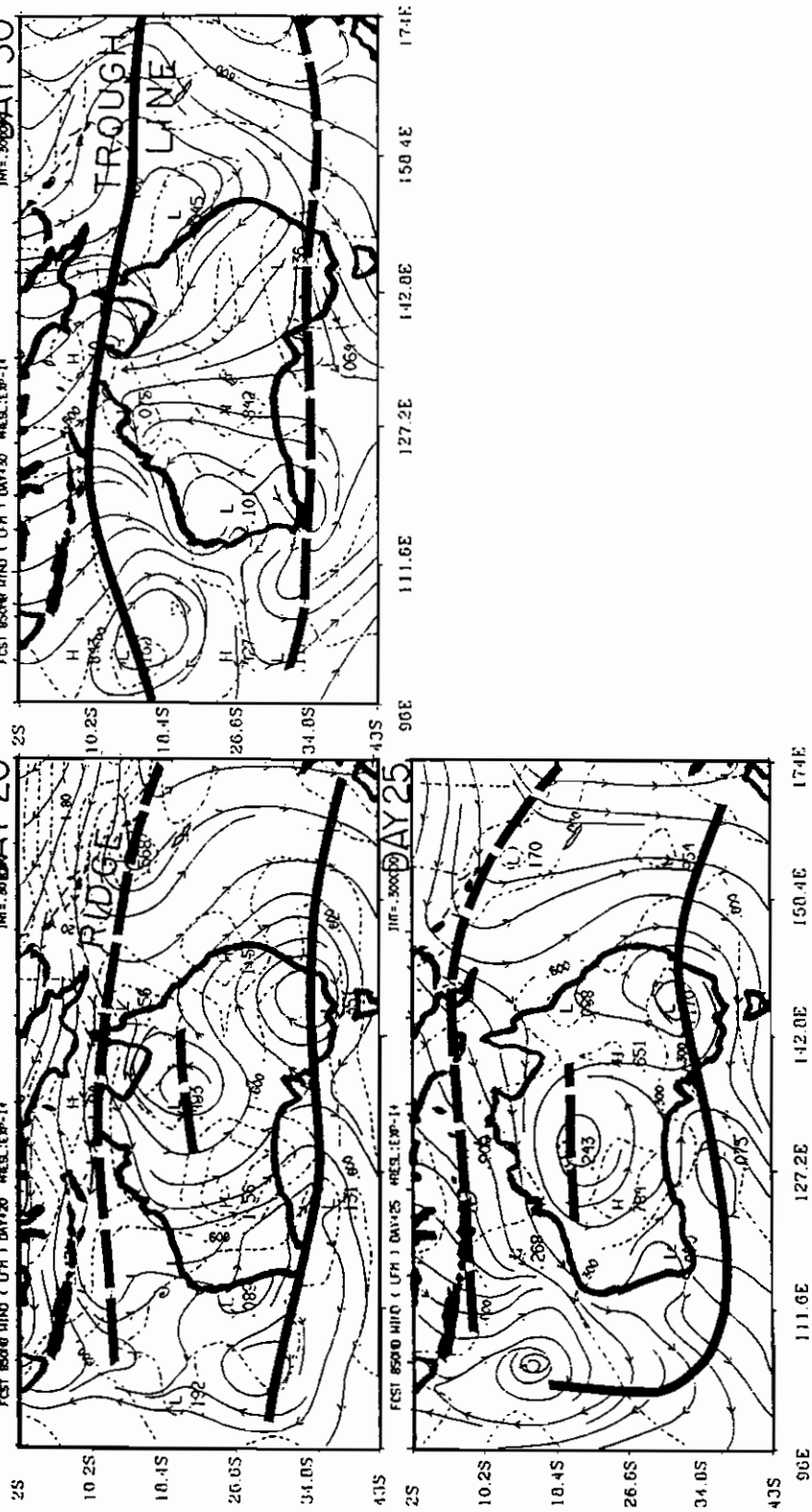

Figure 6. Predicted field at intervals of 5 days of 30–60-day time filtered flow field at 850 hPa from 1 to 30 March 1992 for experiment 1. Streamlines (solid lines) and isotachs (dashed lines) at intervals of 0·3 m s^{-1}. Thick lines are trough lines and thick dashed lines are ridge lines

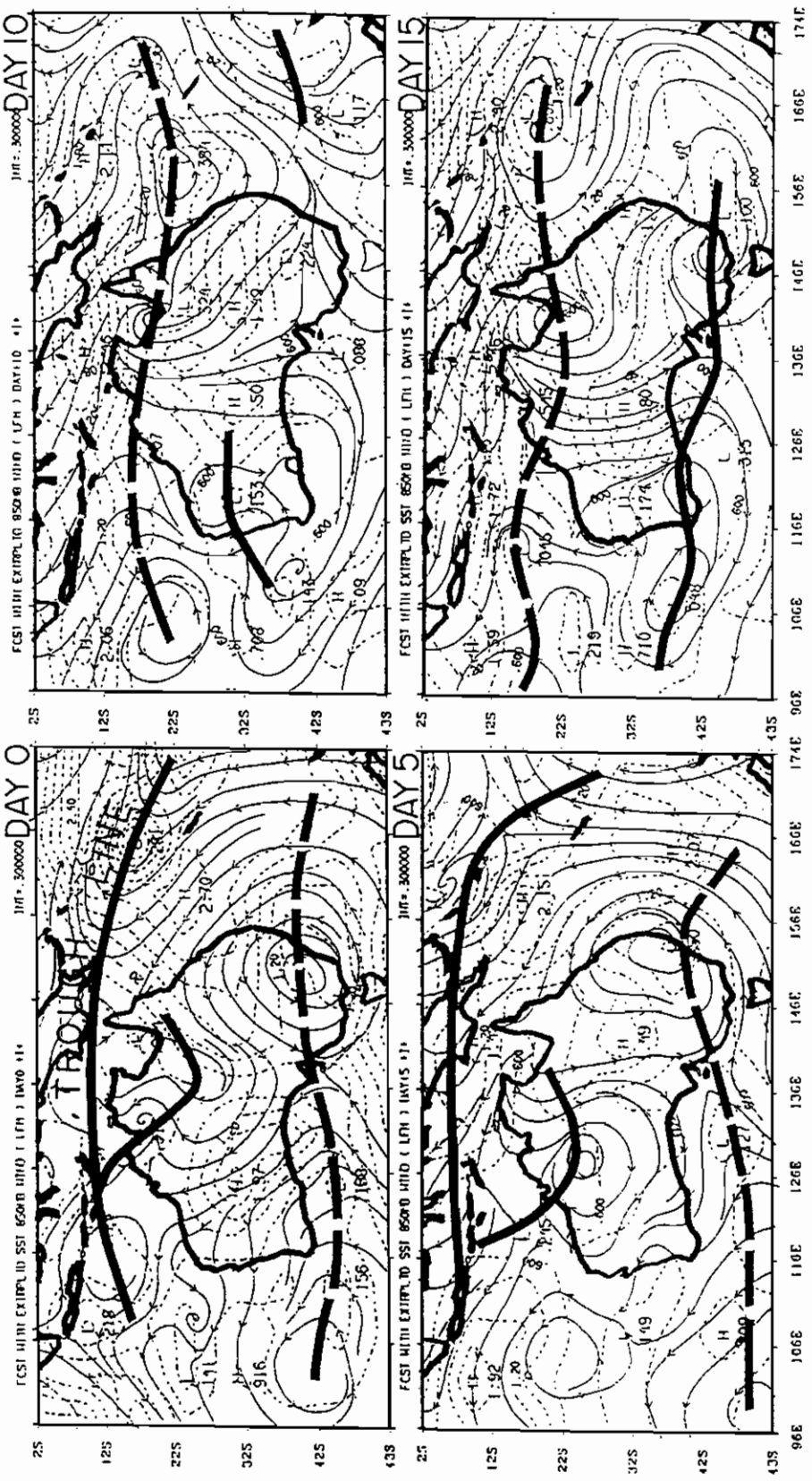
DAY 0
DAY 5
DAY 10
DAY 15
TROUGH
STATE

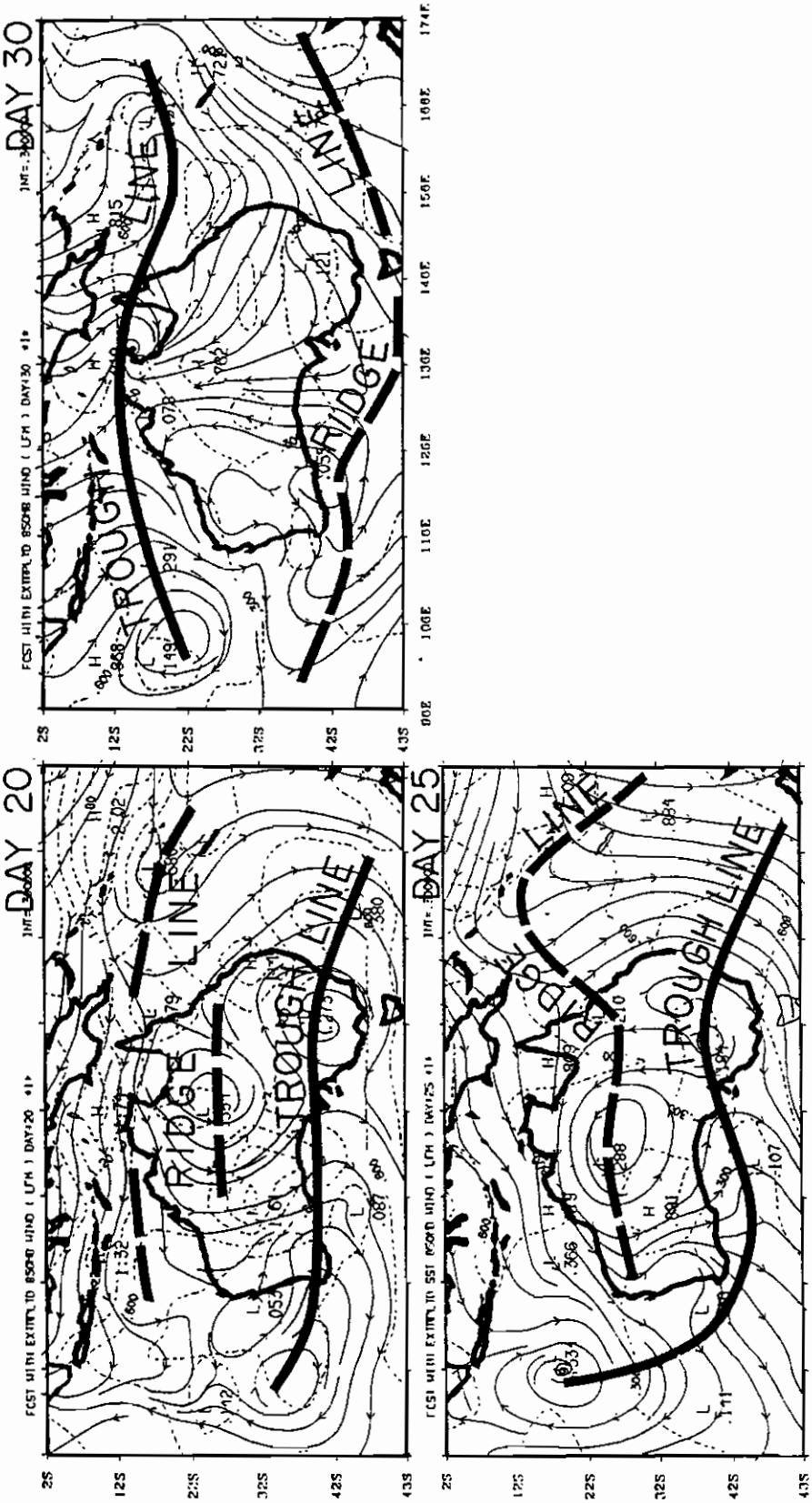

Figure 7. Predicted field at intervals of 5 days of 30–60-day time filtered flow field at 850 hPa from 1 to 30 March 1992 for experiment 2. Streamlines (solid lines) isotachs (dashed lines) at intervals of 0·3 m s^{-1}. Thick lines are trough lines and thick dashed lines are ridge lines

describe slowly varying solutions of the global model. We had felt that the model needed to be spun up to accept a slowly varying time mean plus a low-frequency component. This was addressed by invoking a resilience factor during the initial 5 days of integration. Basically we formulated an equation of this type,

$$\frac{\partial Q}{\partial t} = F$$

by adding a Newtonian term for all the spectral components, i.e.,

$$\frac{\partial Q_l^m}{\partial t} = F_l^m(Q, t) + N\{Q_l^m(t - 120\text{ h}) - Q_l^m\}$$

Here $F_l^m(Q, t)$ denotes the right-hand side of one of the base spectral equations, and l and m are the spectral indices for the order of the associate Legendre functions and the zonal wave numbers respectively. On the right-hand side Q_l^m is a predicted value and $Q_l^m(t - 120\text{ h})$ is a past value, and N is a resilience parameter with a value of 10^{-4} s^{-1}. If the asterisk denotes a forecast without the resilience term, then the finite difference form for the resilience part is written as:

$$\frac{Q_l^m(t + \Delta t) - Q_l^{*m}(t + \Delta t)}{2\Delta t} = N\{Q_l^m(t - 120\text{ h}) - Q_l^m(t + \Delta t)\}$$

or we can write,

$$Q_l^m(t + \Delta t) = \frac{\{Q_l^{m*}(t + \Delta t) + 2\Delta t \times N \times Q_l^m(t - 120\text{ h})\}}{(1 + 2\Delta t N)}$$

As the forecasts proceed, during the first five days, information for the past 5 days are needed to derive $Q_l^m(t - 120\text{ h})$. For this purpose we keep a history of the past values $(t - 120) < 0$ based on the observed time mean plus the low-frequency motion for the desired $(t - 120)$ h. This is an interpolated data file that provides past information for $t - 120$ for $t > 0$. This is involved only for the period $t \leq 120$ h.

With the choice of $N = 10^{-4}$ s^{-1}, we have noted a major improvement in the initial loss of skill during the first 5 days.

PREDICTED LOW FREQUENCY MODES

Here we shall illustrate the results of 30-day forecasts of the two different experiments. It should be noted that during the 30-day integration of the model, some high-frequency motions are generated even though we start with an initial state with no high frequencies. Therefore, the model output is not utilized directly to interpret the circulation patterns of the low-frequency motions. The 30-day wind forecasts at 850 hPa are combined with the previous 120 days of the observed wind, creating a 150-day time series at each of the model grid-points. This 150-day time series is then filtered for the 30–60-day oscillation and the last 30 days of the filtered time series to serve as our forecasts of the low-frequency motions, which are used to interpret the parallel and antiparallel flow patterns. The first of these experiments includes in its initial state, the time mean state, the low-frequency mode, and a prescribed SST anomaly on this time-scale. The SST anomaly is based on observed sea-surface temperatures that include this specified lower boundary condition for the month-long integrations. The low-frequency forecast field obtained from experiment 1 is shown in Figure 6.

As stated earlier the time mean state and the low-frequency mode are described by all the dependent variables at all vertical levels initially. Figure 7 illustrates the 30–60-day forecast field of the second experiment, which differs from the first in its definition of the sea-surface temperature anomaly only, which is extrapolated from its previous state by the method proposed in an earlier section here.

Both of these experiments carried the meridional propagation of the low-frequency mode extremely well. Figures 8 (a and b) illustrates the southward propagation of the ridge and trough lines. As stated earlier these are the zonally averaged latitudinal positions between 96°E and 174°E.

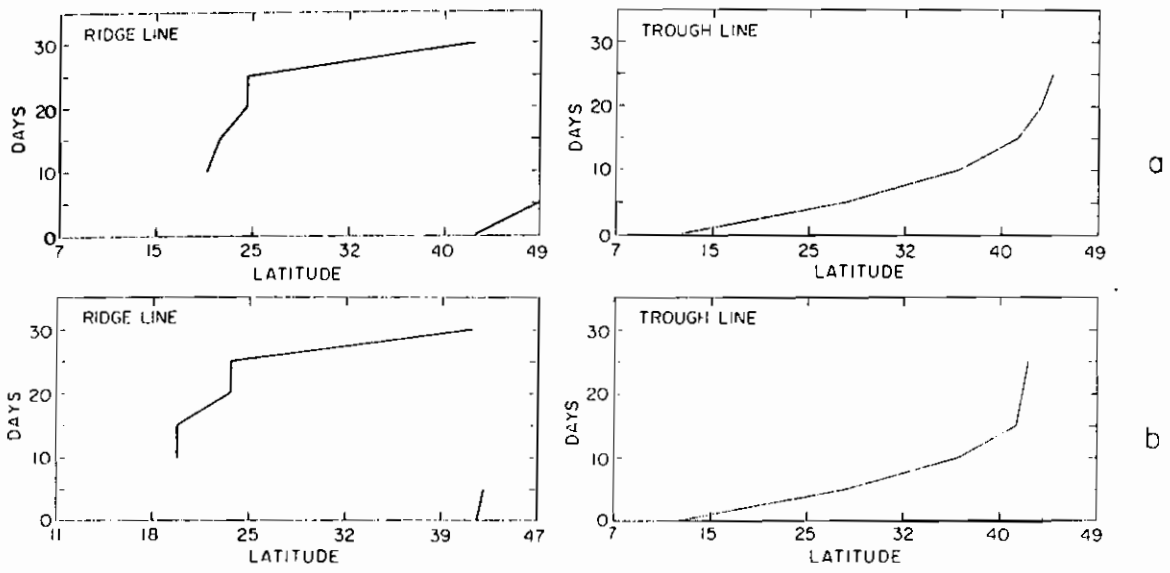

Figure 8. Low frequency (30–60-day) modes of ridge and rough lines, (a) for experiment 1 and (b) for experiment 2

Figures 6 and 7 clearly capture the low-frequency southward propagation of the trough–ridge line. Both experiments show an initial low-frequency trough near 10°S. A part of this trough appears to move close to the Australian desert to around 20°S by day 5. By day 15 the trough moves to around 36°S. The first appearance of a ridge line near 12°S is noted around day 20. A part of this wave moves south to around 20°S by day 25 and to southern Australia by day 30. A quasi-stationary part of the ridge near 12°S at day 20 slowly dissipates in that region between days 25 and 30, and it is replaced by the arrival of a strong trough line by around day 30 of the forecast. These figures compare well with the situation observed in Figure 3(a). Although both the experiments show a rather similar behaviour in the forecast of these gross features, there are some significant differences between the observed and the two experiments, especially in the last 10 days. This is more apparent in the intensity and less in the directions of the flow field. The decay of the anomaly correlations reflect these differences better.

Based on the quality of forecast it can be stated that the lower troposphere climatological cyclonic flow in the ITCZ is enhanced or reduced by the passage of the transient rough or ridge line, producing wet or dry spells respectively. Thus a wet spell can be predicted over Northern Australia to start roughly around 1 March lasting until 5 March as the low-frequency trough propagates southward. A dry spell over Northern Australia can be predicted to begin from around 10 March lasting until 25 March with the southward passage of the ridge line. By the end of the month we see the beginning of another wet spell.

The observed precipitation charts illustrated in Figure 9 indicates the wet and dry spells of the monsoon over Northern Australia. In these rainfall charts, shown at intervals of every 5 days, we clearly see a wet period covering the latitude belt 10°–20°S during the 1 March to 2 March period. Rainfall is expressed in units of mm day^{-1}, and the maximum rainfall is of the order of 30 mm day^{-1}. In contrast, when we examine a period such as 21 March to 22 March, this latitude belt appears to be generally less than 10 mm day^{-1}. At the last part of the month the wet period around 31 March to 1 April is characterized by rainfall amounts of the order of 28 mm day^{-1} in the latitude belt 10°–20°S. It conforms well with our prediction of the circulation anomalies. As suggested earlier, the method described in this study gives an outlook forecast of the dry and wet spells of the monsoon in Northern Australia.

ANOMALY CORRELATIONS

Figures 10 and 11 illustrate the anomaly correlations of the 850 hPa for experiments 1 and 2. The first of these is not entirely a predictive experiment because it uses SST data from the future, whereas the second experiment is

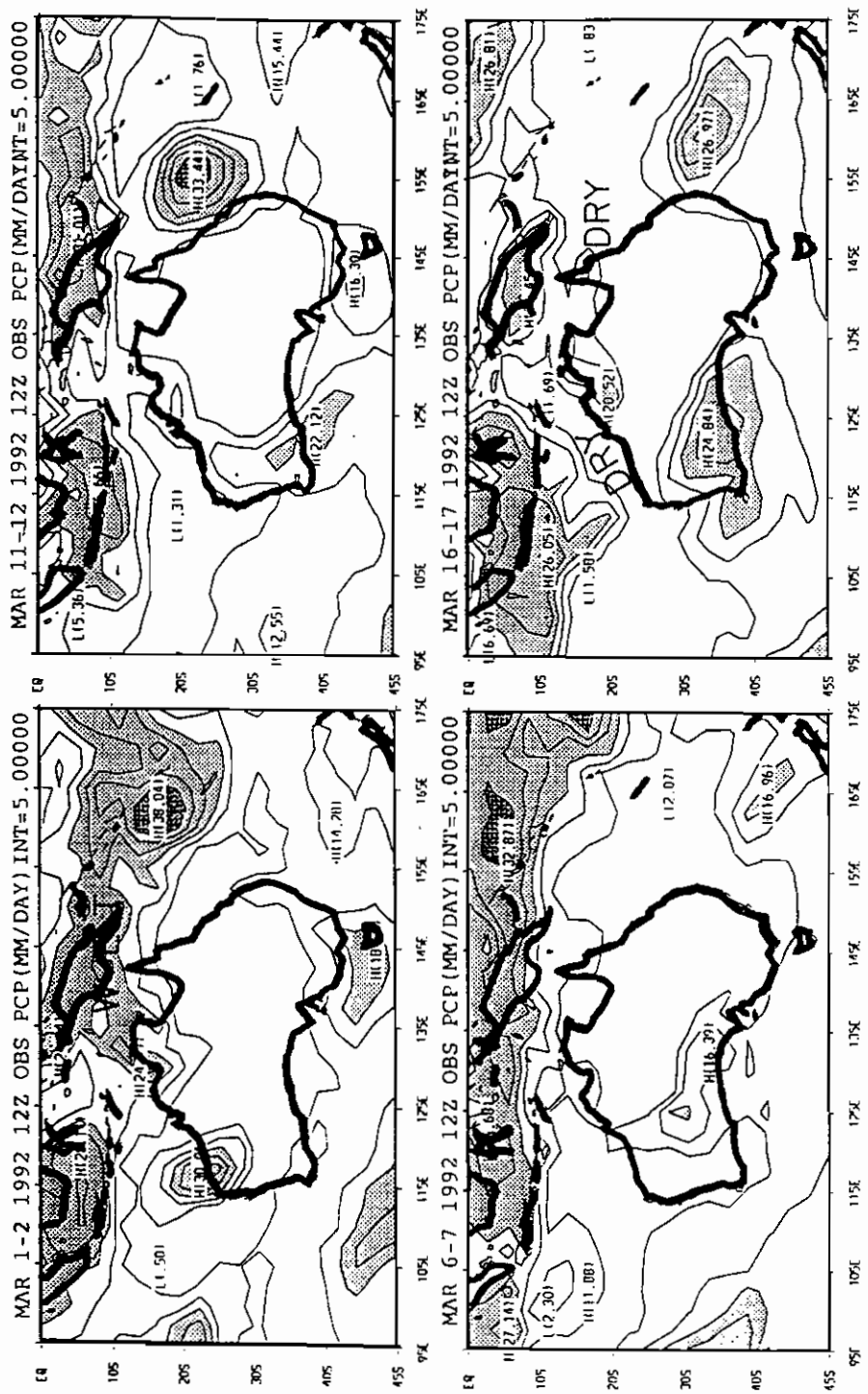
MAR 1-2 1992 12Z OBS PCP(MM/DAY) INT=5.00000
MAR 11-12 1992 12Z OBS PCP(MM/DAYNT=5.00000
MAR 6-7 1992 12Z OBS PCP(MM/DAY) INT=5.00000
MAR 16-17 1992 12Z OBS PCP(MM/DAYNT=5.00000
DRY
DRY

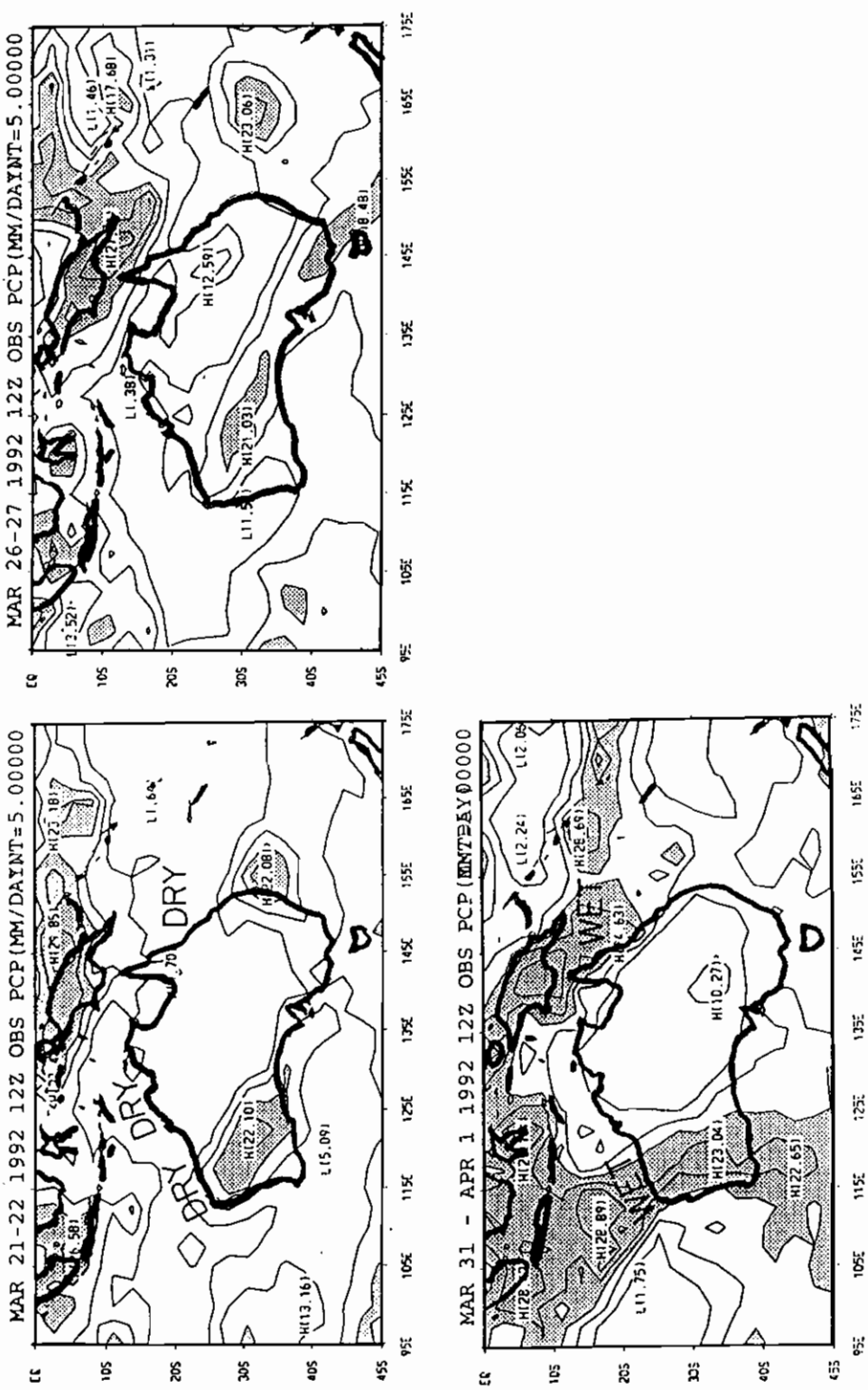

Figure 9. Observed 24-h rainfall totals (mm day^{-1}) through the month of March 1992, at intervals of 5 days. Interval of isopleths are 5·00 mm day^{-1}

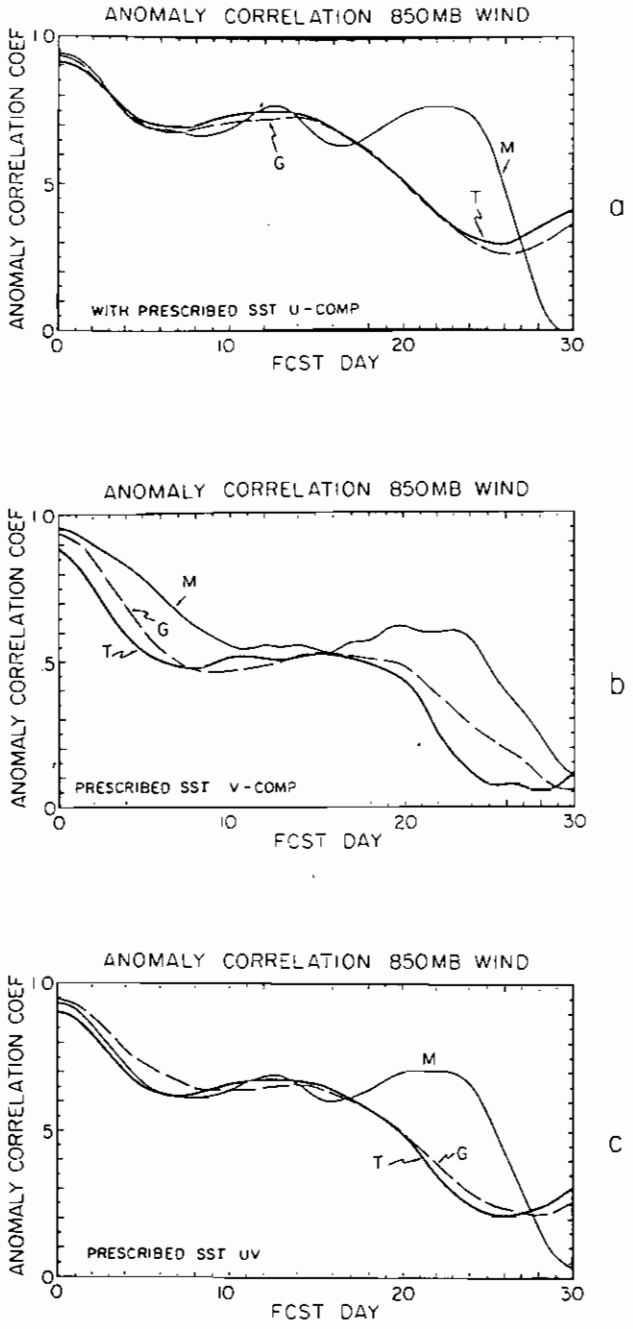

Figure 10. Anomaly correlation of (a) u component, (b) v component, and (c) total wind (uv) for experiment 1

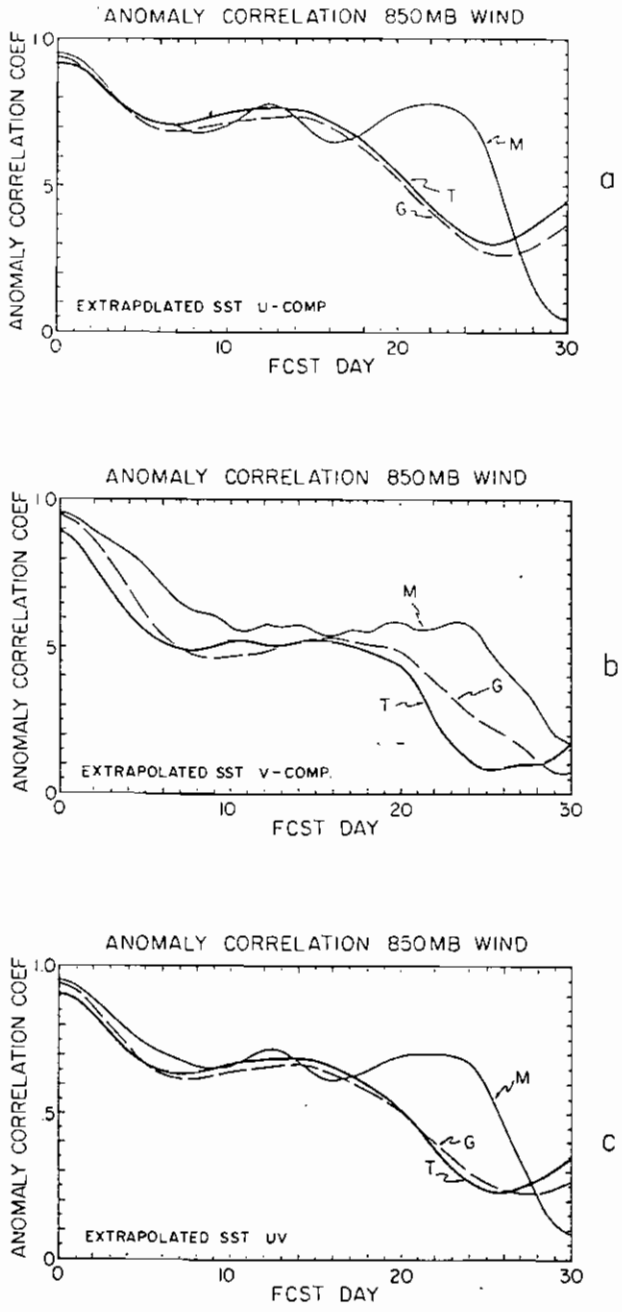

Figure 11. Anomaly correlation of (a) u component, (b) v component, and (c) total wind (uv) for experiment 2

entirely a predictive experiment. In these illustrations panels a, b, and c, respectively, show the anomaly correlations for the 30-day forecast for the zonal wind, the meridional wind, and the total wind respectively. The results were averaged over three domains. A monsoon domain, designated by the letter M, covers an area bounded by longitude 96° to 174°E and latitude 2° to 42°S. The results for a tropical domain, labelled T, cover the latitude belt between 30°S and 30°N. The letter G denotes the results over the entire globe. Basically we find higher skill in the prediction of zonal wind on the time-scale of 30–60-days. These anomaly correlations are of the order of 0 · 7 through to day 25 of the forecasts. The meridional wind is not handled as well by the proposed modelling approach. The skill is of the order of 0·55–0·50 through to roughly 25 days. The skill of the total wind is of the order of 0·65 through to roughly 25 days of forecast. A sharp loss of skill is noted over the Australian monsoon domain beyond 25 days. That loss is attributed to a rapid growth of higher frequencies that seem to contaminate the lower frequency motions (Krishnamurti *et al.*, 1992b). The skill over the monsoon region appears to be higher than that over the entire tropical belt and over the globe. The 30–60-day oscillations are a characteristic feature of the monsoon region (Krishnamurti and Gadgil, 1985). The results with the prescribed and the extrapolated SST anomalies are nearly identical. This shows that the short-period extrapolation nearly captures the salient oseillation of the SST anomaly on this time-scale. Overall, the forecast of the circulations on this time-scale are very reasonable to about 25 days. It should be noted that even though a sharp drop in skill is noted between days 25 and 30, the location of the predicted trough is closely predicted to that based on the observed wind. The low anomaly conclusion implies a degradation of the amplitude of the low-frequency motions during the last 5 days of integration. The useful prediction of the circulation geometry is still quite useful for providing an outlook forecast of the dry and wet spell over the northern Australian region to roughly 30 days.

CONCLUDING REMARKS

In this study we have demonstrated the possibility for month-long forecasts of dry and wet spells of the Australian monsoon based on the passage of low-frequency trough and ridge systems. This study is analogous to our previous efforts to predict the monsoon activity over India and China. The procedure entails a prediction with a global model where a time mean state and a low-frequency state of the atmosphere define the initial state. Higher frequencies are excluded initially; they evolve slowly and contaminate the overall fields. However, a useful projection of the passage of the low-frequency motions through one cycle (roughly 30 days) appears to be possible. This procedure, at best, seems to provide only an outlook forecast. In this experiment the initial period was characterized by a wet spell over Northern Australia and the region to its immediate north. The month-long forecast calls for the superpositions of an anticyclonic circulation of the time mean flow, thus weakening the cyclonic flow over the ITCZ of this region and suggesting below normal monsoon activity. That period lasted roughly from day 10 to day 25 of the forecast and coincided with the observed dry spell of the monsoon over Northern Australia. Furthermore, the forecast called for a superposition of a low-frequency cyclonic circulation anomaly over the time mean cyclonic circulation of the ITCZ at the end of the month-long forecast. The start of the wet spell appeared to coincide closely with the superposition of the cyclonic circulation systems on these two time-scales, i.e. around 30 March. Rain-producing systems tend to form within the climatological lower tropospheric cyclonic circulation systems in the tropics. It is this aspect of tropical rainfall behaviour that, we believe, makes this a useful outlook forecast.

In these experiments, the sea-surface temperatures (SST) need to be prescribed during the month-long integrations. The SST field contains a climatological part and an anomaly on the time-scale of 30–60-days. Two experiments were carried out, where the SST anomaly was based on observations and another where the SST anomalies were obtained by a Fourier extrapolation of past anomalies prior to the initial state. Results from both experiments were closely comparable. The former approach is not entirely predictive because the future values of SST anomalies based on observation were used. The second approach is entirely predictive.

The skill of these month-long circulation forecasts was monitored from the anomaly correlations of the predicted low-frequency motion field. The proposed modelling approach appears to handle the prediction of the low-frequency motions at 850 hPa to levels of the order of 0·7 to almost 25 days of integration. As the higher frequency motions evolve, the forecasts begin to exhibit a deterioration of the low-frequency motions around the end of the

month. The experiments shown here were carried out at a low horizontal resolution, i.e. 21 waves triangular truncation (T21). Experiments carried out at higher horizontal resolutions, such as T42, exhibited a more rapid decay of skill owing to the rapid growth of higher frequency motions. Further work is needed to parameterize the effects of the higher frequencies. Some pioneering work is currently being done by Stewart (1994) to explore these issues.

ACKNOWLEDGEMENTS

The research reported here was supported by NOAA grant NA16RC0358-02 and by NSF grant ATM 8812053. The computations for this work were carried out on the CRAY/MP at Florida State University's Supercomputer Computational Research Institute supported by the Department of Energy.

REFERENCES

Asselin, R. 1972. 'Frequency filter for time integrations', *Mon. Wea. Rev.*, **100**, 487–490.

Atkinson, G. D. 1971. *Forecasters' Guide to Tropical Meteorology*, Airweather Service (MAC) United States Air Foree.

Comeaux, J. L. 1991. The origin and structure of the low-frequency modes. MS thesis, Florida State University, Tallahassee, FL, 54 pp.

Dastoor, A. and Krishnamurti, T. N. 1991. 'The landfall and structure of a tropical cyelone: the sensitivity of model predietions to soil moisture parameterization', *Bound. Layer Meteorol.*, **55**, 345–380.

Diaz, H. F., Bradley, R. S. and Eishehield, J. K. 1989. 'Precipitation fluctuations over global land areas since the late 1800s', *J. Geophys. Res.*, **94**, 1195–1210.

Harshvardan, xxx and Corsetti, T. G. 1984. *Longwave Parameterization for the UCLA/GLAS GCM*. NASA Technical Memorandum 86072, Goddard Space Flight Center, Greenbelt, MD.

Kanamitsu, M. 1975. *On Numerical Prediction over a Global Tropical Belt*. Report no. 75-1, Department of Meteorology, Florida State University, Tallahassee, FL, 282 pp.

Kanamitsu, M., Tada, K., Kudo, K., Sato, N. and Isa, S. 1983. 'Description of the JMA operational spectra model', *J. Meteorol. Soc. Jpn*, **61**, 812–828.

Kitade, T. 1983. 'Nonlinear normal mode initialization with physics', *Mon. Wea. Rev.*, **111**, 2194–2213.

Krishnamurti, T. N. and Gadgil, S. 1985. 'On the structure of the 30–50 day mode at 850 mb during MONEX', *J. Atmos. Sci.*, **39**, 2088–2095.

Krishnamurti, T. N., Low-Nam, S. and Pasch, R. 1983. 'Cumulus parameterization and rainfall rates II', *Mon. Wea. Rev.*, **111**, 815–828.

Krishnamurti, T. N., Bedi, H. S., Heckley, W. and Ingles, K. 1988. 'Reduction of the spin up time for evaporation and precipitation in a spectral model', *Mon. Wea. Rev.*, **116**, 907–920.

Krishnamurti, T. N., Subramaniam, M., Oosterhof, D. and Daughenbaugh, G. 1990. 'On the predictability of low-frequency modes', *J. Meteorol. Atmos. Phys.*, **44**, 63–84.

Krishnamurti, T. N., Sinha, M. C., Krishnamurti, R., Oosterhof, D. and Comeaux, J. 1992a. 'Angular momentum, length of day and monsoonal low-frequency mode', *J. Meteorol. Soc. Jpn*, **xx**, 131--166.

Krishnamurti, T. N., Subramaniam, M., Daughenbaugh, G., Oosterhof, D. and Xue, J. 1992b. 'One month forecasts of wet and dry spells of the monsoon', *Mon. Wea. Rev.*, **120**, 1191–1223.

Lacis, A. A. and Hansen, J. E. 1974. 'A parameterization for the absorption of solar radiation in the earth's atmosphere', *J. Atmos. Sci.*, **31**, 118–133.

Louis, J. F. 1979. 'A parametric model of vertieal eddy fluxes in the atmosphere', *Bound. Layer Meteorol.*, **17**, 187–202.

Stewart, A. D. 1994. 'Predictability of low frequency planetary waves in a simple low resolution model', *Mon. Wea. Rev.*, in press.

Stringer, 1991. 'Monitoring the active/inactive cycle of the Australian summer monsoon', *Proceedings of a WMO Conference on Monsoon*, Kuala Lumpur, Malaysia.

Tiedke, M. and Slingo, J. 1985. *Development of the Operational Parameterization Scheme*. ECMWF Research Department, Technical Memorandum 108, ECMWF, Reading, 38 pp.

Troup, A. J. 1961. 'Variations in upper tropospheric flow associated with the onset of Australian Summer Monsoon', *Indian J. Meteorol. Geophys.*, **12**, 217–230.